Design of a Batch Reactor for the Conversion of 500g Microalgae Biomass to Biocrude by Hydrothermal Liquefaction

Ikhazuangbe[a,b,*], Prosper Monday Ohien, Eboibi[b,d] Blessing Elo, Amabogha[b,d], Blessing, Orugba[b], Oghenero Henry, Ikalumhe[e], Wilfred Onoshiorena & Agarri[c,d], Samuel Enahoro
[a]Chemical Engineering Department, Edo State University Uzairue, Nigeria.
[b]Chemical Engineering Department, Delta State University, Oleh Campus, Nigeria.
[c]Chemical Engineering Department, Ladoke Akintola University, Ugbomosho, Nigeria.
[d]Chemical Engineering Department, Federal University Otuoke, Bayelsa State, Nigeria.
[e]Mechanical Engineering Department, Edo State University Uzairue, Nigeria.
Corresponding author: email: ikhazuangbe.prosper@edouniversity.edu.ng

DOI: 10.56201/ijemt.v9.no3.2023.pg1.14

ABSTRACT

Biocrude is a viable renewable source of energy and its production is gaining more attention globally. This work entails design of a batch reactor for the conversion of $500g$ *microalgae biomass to biocrude by hydrothermal liquefaction. The material and energy balances of the reactor were calculated and the percentage weights of the various products (biogas, biocrude, liquid phase and biochar) used for the design with a ratio of 4:1 for the solvent and microalgae biomass, were 5wt%, 50wt%, 30wt% and 15wt% respectively. The heat capacity of triglyceride used in the design, show that the maximum amount of energy required in the unit is* $1096W$*. The reactor volume, height, wall thickness, thickness of the flat end and the thickness of the insulation material were designed as* $4170cm^3$*, 240mm,* $2.2mm$*, 5.5mm and* $2mm$ *respectively. The reactor is designed to be operationally safe and economically viable, with a total cost of fabrication estimated at two hundred and fifty eight thousand, two hundred naira only (N208,200).*

KEYWORDS: *Biocrude Reactor, Design, Hydrothermal Liquefaction, Microalgae, Renewable Energy*

I. INTRODUCTION

Attention all over the world in recent years is shifting towards energy from renewable resources such as microalgae because of the increasing energy consumption and to achieve climate goal (Mahima *et al*, 2021; Chen and Quinn, 2021). Microalgae look promising as bioenergy resource because of their ability to grow in a saline, degrade water bodies, their prolific growth rate, ability to utilize waste CO_2, their high lipid productivity and non-arable land can use for their cultivation (Vardon *et al*, 2012; Chen and Quinn, 2021). When these microalgae are harvested, their biomass can be converted into fuels by hydrothermal liquefaction operation (Chen and Quinn, 2021). Hydrothermal liquefaction can convert dry or wet biomass to biocrude, thereby overcoming the problem of energy consumption involved in dewatering usually encountered in the use of pyrolysis (Le *et al*, 2019; SundarRajan *et al*, 2021), gasification (Xu *et al*, 2019) and transesterification

(Eboibi *et al,* 2015) methods. Therefore, extra energy is not expended to dry the biomass and this hydrothermal liquefaction operation is not highly corrosive to the reactor (SundarRajan *et al,* 2021). Previous reports investigated the effects of residence time, catalyst, solid concentration, temperature, solvent and the strain of microalgae on the biocrude production quality and yield (Eboibi *et al,* 2015). Hydrothermal liquefaction operation is specifically carried out at a process temperature range of $200\ to\ 380℃$ (Tian *et al,* 2014), high pressure range of $2\ to\ 25bar$ (Eboibi, 2019) and residence time range of about 5 to 120 minute in the presence of water (Barreiro *et al,* 2014). This operation can be carried out with or without the use of catalyst (Xu *et al,* 2019).

The main by-products of the hydrothermal liquefaction operation are aqueous phase, gases and solid residue, while the primary product is biocrude (Kumar *et al,* 2018).

Several researchers, who worked on microalgae biomass hydrothermal liquefaction for the production of biocrude, did not actually design the reactors they used for the operation; hence, the data about the configuration of the biocrude reactor is scanty. Jazrawi *et al,* (2015) used a small-scale batch reactor of about 20mL, 120mm length, 0.75inch outer diameter made of stainless steel 316 of 1.65mm wall thickness. Though, they did not report in their work that the batch reactor was designed and produced by them. Kandasamy *et al,* (2021) reported that they used a 50mL capacity batch reactor, built with stainless steel 316 for the hydrothermal liquefaction, but the design of the reactor was not stated in their work. Hoang *et al,* (2021) used a 3.2 liters ($3200cm^3$) reactor to produce biocrude using $350g$ lignocelluloses biomass. Wang *et al,* (2021) used a batch reactor of about 50mL internal volume, produced with stainless steel 316, fitted with electric furnace and a rotary evaporator. They reported that the maximum temperature and pressure the equipment can withstand is $400℃$ and $60bar$. Wang *et al,* (2018) used 1800ml stainless steel reactor for the conversion of 120g of NAS and 480g of water for the production of biocrude. They operated the reactor for about 30min but did not report the operating temperature. Barreiro *et al,* (2015) used 10ml stainless steel reactor, filled to about70% with algae-water at a ratio of 1:10. Costarizo *et al,* (2015) carried out their reaction in a 75ml reactor with 7g of algae and 32g deionized water at different temperature with 225ºC as maximum and for a maximum of 21min.

In similar field of producing biocrude from the biomass of microalgae by hydrothermal liquefaction, this work is set to provide detailed process and equipment design of a laboratory-scale batch reactor for the production of biocrude from $500g$ microalgae biomass by hydrothermal liquefaction.

II. MICROALGAE

These are microscopic photosynthetic protists, which do not have roots, stem, leaves or vascular tissue, but floats as plankton (Song *et al,* 2015). They live in wide range of environmental conditions (temperature, pH, salinity or light intensity), because of the different physiological systems they have developed, which allow them to adapt (Geada *et al,* 2017).

Microalgae consist mainly of proteins, carbohydrates and lipids. The main component of the biomass of microalgae that transform into biocrude is lipid. Lipids easily hydrolyze during hydrothermal liquefaction to glycerol and higher fatty acids. Lipids do not transform at all into the solid phase (Hao *et al,* 2021). Lipids exist in the form of triglyceride which has low dielectric constant that quickly undergoes noncatalytic hydrolysis to generate higher fatty acids and glycerol under hydrothermal liquefaction conditions (Hu *et al,* 2019; Hao *et al,* 2021). They contain glycerol backbone connected to three free fatty acids. At subcritical condition under which biocrude is produced, triglycerides easily decompose to form free fatty acids and glycerol (Hu *et*

*al,*2019). Lipids which form the main source of light components in biocrude do not get converted by hydrothermal liquefaction at all into the solid phase. Its contributions to heavy components of biocrude depend on the temperature. Lipids contribute more at low temperatures, but at higher temperature, their contribution is similar to that of proteins (Hao *et al,* 2021). Specific heat capacity, which is a thermo-physical property of food, is an essential component to energy balance in process design (Zhu *et al,* 2018). The specific heat capacities of triacylglcerols of different forms according to Zhu *et al*, (2018) are listed in Table 1.

Table 1 Specific heat Capacity of Triacylglycerols

Triacyglcerols	Specific heat capacity kJ/kg
Tristearin	1.938
Triolein	1.886
Trilinolein	1.813
Trilinolenin	1.765

A. Hydrothermal Liquefaction Reactor

A reactor is an apparatus or vessel in which reaction proceeds in a controlled manner. Reactor design helps to know the size and type of reactor to be engaged in an operation. This is because the conditions in the rector may vary their position as well as time. This may likely encounter some difficulties because the composition and temperature of the reacting species may change from point to point within the reactor (Octave, 2008).

Generally, reactors can either be batch or continuous-flow reactors. In small scale production, manufacturing of expensive products, for testing new processes, and for manufacturing operations that are difficult to convert by continuous operation, batch reactors are used. The batch reactor can be loaded through the holes at the top and has the advantage of high conversion when the reactants are left in the reactor for a long of time. Batch reactor however, has high cost of labor per batch operation, variation of products from batch to batch, and the difficulty of been used for large-scale production (Fogler, 2012). A mole balance on specie A, at any time t, is expressed as follows:

$$\left[Rate\ of\ flow\ of\ A\ into\ the\ system\ (\frac{mole}{tme})\right] - \left[Rate\ of flow of A\ out\ of\ the\ system\ (\frac{mole}{time})\right] + \left[Rate\ of\ disappearance\ of A\ by\ chemical\ reaction\ with\ the\ system\ (\frac{mole}{time})\right] - \left[Rate\ of\ accumulation\ of A\ within\ the\ system\ (\frac{mole}{time})\right] \quad (1)$$

But in a batch reactor, Flow input = 0; flow output = 0

Therefore,

0 = rate of disappearance + rate of accumulation (2)

Rate of disappearance of A = $-r_A$V

Where

By implication, rate of disappearance = $\frac{moles\ of\ A\ reacting}{(time)\ (volume\ of\ fluid)}$ x volume of fluid

= $\frac{moles\ of\ A\ reacting}{time}$

Rate of accumulation = $\frac{dN_A}{dt}$ (3)

But $N_A = N_{Ao}(1 - X_A)$

$$\frac{dN_A}{dt} = \frac{d(N_{Ao}(1- X_A)}{dt} \quad (4)$$

But N_{AO} is the initial number of moles fed into the reactor, therefore N_{AO} if constant with respect to time;

Therefore, equation (4) becomes

$$\frac{dN_A}{dt} = 0 - \frac{N_{AO}dX_A}{dt}$$

$$= \frac{-N_{AO}dX_A}{dt} \quad (5)$$

Substituting equations (3) and (5) into (2)

$$0 = -r_A V - \frac{-N_{AO}dX_A}{dt}$$

$$-r_A V = \frac{N_{AO}dX_A}{dt} \quad (6)$$

This is the batch reactor design equation in differential form, where $-r_A$= rate of the reaction of reactant A, V = volume of the reactor and X_A = mass fraction of reactant A

Therefore, volume of the biomass reactor is obtained as:

$$V = \frac{-N_{AO}dX_A}{r_A dt}$$

$$V = \frac{N_{AO}\,X_A}{t\,kC_A} \quad (7)$$

Where $-r_A = kC_A$

1) Reactor Wall Thickness

The thickness of the reactor wall is very significant and must be designed to resist the internal pressure buildup, having safety allowance for corrosion and other mechanical allowances for pressure gauge, safety valve and pipe threads. Process batch reactors or cylindrical reactors can normally be considered as thin cylinders; but high-pressure pipes or reactors such as bioreactor for the hydrothermal liquefaction of biocrude, are classified as thick cylinders and must be given special consideration (Aprilla *et al*, 2023). A vessel or reactor must be designed to withstand the maximum working pressure to which it is likely to be subjected during the operation and a maximum allowable pressure of 10% is set in practice (Towler and Sinnott, 2008). The formula for the evaluation of the thickness of the cylindrical reactor is as obtained for ASME B31.3 code:

$$t_m = t_p + C$$

$$t_p = \frac{P\,d}{2\,(S\,E - P\,\gamma)}$$

Therefore,

$$t_m = \frac{P\,d}{2\,(S\,E - P\,\gamma)} + C \quad (8)$$

Where t_m is the minimum required thickness; t_p is the pressure design thickness; C is the sum of mechanical allowances (thread depth) and corrosion allowances; P is the internal design gauge pressure, lb/in^2 (or N/mm^2); d is the pipe inner diameter; S is the basic allowable stress for pipe material, lb/in^2 (or N/mm^2); E is the casting quality factor; γ is the temperature coefficient (0.6) (Sinnott, 2005).

2) The Flat Ends of the Reactor

The flat end of the reactor that requires special attention is the top where the sensing devices will be mounted. The cost of fabricating the flat end is low, but these flat ends are not in structurally

efficient form, and very high pressures require thick plate. Therefore, the design equations used for the flat plate thickness determination are based on their stresses analysis, as Table 2 shows various design stresses for plates (Towler and Sinnott, 2008). The thickness required for flat ends will depend on the degree of constraint at the plate periphery.
The minimum thickness required for a flat end is given by:

$$t_m = C_p D_e \sqrt{\frac{P_i}{f}} \quad (9)$$

Where C_p is the design constant and is dependent on the edge constraint, D_e is the internal plate diameter, f is the design stress. Any consistent set of units can be used (Sinnott, 2005).

Table 2 Typical Plate Design Stresses

`Material	Tensile strength N/mm^2	Design stresses at temperature ^{o}C (N/mm^2)									
		0 - 50	100	150	200	250	300	350	400	450	500
Carbon steel	360	135	125	115	105	95	85	80	70		
Carbon-Manganese steel	460	180	170	150	140	130	115	105	100		
Carbon-Molybdenum steel	450	180	170	145	140	130	120	110	110		
Low alloy steel (Ni, Cr, Mo, V)	550	240	240	240	240	240	235	230	220	190	170
Stainless steel 18Cr/8Ni (304)	510	165	145	130	115	110	105	100	100	95	90
Stainless steel 18Cr/8Ni (321)	540	165	150	140	135	130	130	125	125	120	115
Stainless steel 18Cr/8Ni (316)	520	175	150	135	120	115	110	105	105	100	95

3) Insulation of the reactor
These are materials used for covering other materials to reduce heat, sound or electricity loss or entrance when in contact with an object or in a radiative range of influence (Rehan, 2020). A wide range of these materials used for insulation exist, however, the most common types used for loose-fill include: fiberglass, cellulose and wool. Selection of material to be used for insulation is based on their initial cost, their effectiveness, durability, adaptability of its form to the material that will be insulated. Economically, it may be better to choose an insulation material with a lower thermal

conductivity than increasing the thickness of the insulation of a material of higher thermal conductivity in the hold walls (Etuk *et al*,2020).
Fiberglass insulation will be used in this research work because of its high resistance to microbiological attack, high resistance to fire attack, good resistance to most chemicals, high heat resistance, low thermal conductivity and its availability in a variety of presentations. Table 2 shows the thermal conductivity of different types of fiberglass (Zaid, 2020).

Table 3 Thermal Conductivity and Density values at $0^{\circ}C$ of Fiberglass

Type	Density $\boldsymbol{kg/m^3}$	Thermal conductivity $(\boldsymbol{W/m}^{\circ}C)$
Type I	10 – 18	0.044
Type II	19 – 30	0.037
Type III	31 – 45	0.034
Type IV	46 – 65	0.033
Type V	66 – 90	0.033
Type VI	91	0.036
Glass fiber, resin bonded	64 – 144	0.036

The reactor has a cylindrical pipe shape, therefore the heat conduction in this system is in the radial direction and the area normal to flow varies with distance (Iyagba, 2008). Therefore, applying Fourier's law for a cylindrical system:

$$Q = \frac{-2\pi L k (\Delta T)}{ln\frac{r_o}{r_i}} \quad (10)$$

Where Q is the rate of heat loss, L is the length or height of the cylinder, ΔT is the temperature difference, while r_o and r_i are the outer and inner radius respectively. For a cylindrical system with insulation, equation (10) will become:

$$Q = \frac{-2\pi L (\Delta T)}{\frac{1}{k_1} ln\frac{r_2}{r_1} + \frac{1}{k_2} \ln\frac{r_3}{r_2}} \quad (11)$$

Where r_1 and r_2 are the inner and outer radius of the cylinder, r_3 is the outer radius of the insulator, k_1 is the heat transfer coefficient of thermal conductivity of the cylinder, k_2 is the thermal conductivity of insulator.

4) The Reactor Stirrer with Impellers

This is a device which helps to provide homogeneity of heat around the biomass inside the reactor. The types of available stirrer are paddle, turbine, anchor and propeller, but the propeller or impeller type of stirrer is better in viscous and corrosive materials. The expressions for designing the various parameters of an impeller are presented in Table 4 (Aprilla *et al*, 2023).

Table 4 Properties of the Stirrer

Section	Parameters	Equation
Stirrer	Impeller diameter (Da)	Da = di x 0.5
	Impeller height from the bottom of the vessel (Zi)	Zi = 1/3 x di
	Impeller width (W)	W = 0.2 x Da
	Impeller length (L)	L = 1/4 x Da

III. MATERIAL AND ENERGY BALANCES

Steady state condition will be assumed for the reactor and it will be assumed also that there is no chemical reaction.

A. Material balance

The material balance for the configuration will be expressed as:

Basis: 500g of microalgae biomass

$$Material\ input + rate\ of\ generation = material\ output + rate\ of\ disappearance \quad (12)$$

At steady state, since there is no chemical reaction and accumulation is zero,

$$Material\ input = material\ output \quad (13)$$

Therefore,

$$Biomass = gas\ phase\ (g) + solid\ residue\ (g) + biocrude\ (g) + aqueous\ phase\ (g) \quad (14)$$

B. Energy balance

Using the equation of heat balance, Q = $mc_p\theta$, where m is the mass of the biomass, c_p is the specific heat capacity of the Tristearin (Table 1), a form of pure Triacylglycerols, a saturated lipid (Zhu *et al*, 2018).

Q = $mc_p\theta$

= 2500g x $1.938\frac{KJ}{kg℃}$ x $(400 - 30)℃$

= 2.5kg x $1.938\frac{KJ}{kg℃}$ x $370℃$

= 1792.7 kJ

The operational amount of heat required for the hydrothermal liquefaction is 1792.7kJ or 996W. But the design heat required for the hydrothermal liquefaction is 10% of the operational heat (Towler and Sinnott, 2008). Therefore,

Q = 996 + 99.6

= 1096W

C. Reactor design

Lipids present in microalgae, are the major components that transforms into bio-crude. Chen *et al.*, (2018) reported in their work that the lipid content of microalgae ranges from 20 – 50%, depending on the microalgae species, Spirulina 38.6% (Song *et al*, 2015), Chlorella 39.4% (Tian *et al*, 2022), Dunaliella 44.63% (Song *et al*, 2015) and Nanochloropsis 42.67% (Song *et al*, 2015). The feed stream to the batch reactor will be taken to be operating at an optimal temperature

condition (Amiri and Arabian, 2016). Therefore, average mass fraction $X_A$of biocrude yield from microalgae will be, 0.4133. Using equation (7),

Volume of the reactor V = $\frac{N_{Ao}\, X_A}{t.k.C_A}$

Where k = maximal hydrolysis rate of lipid Linoleic acid $0.0095\ min^{-1}$ (Chen *et al*, 2018; Joelianingsih *et al*, 2014), t = time taken for the HTL operation, and X_A = the mass fraction of lipids that convert to biocrude from biomass.

N_{AO} = $\frac{\text{500g of the microalgae biomass} \times \text{mole fraction of the lipids in the microalgae biomass}}{molecular\ weight\ of\ the\ lipid}$

Therefore $N_{AO} = \frac{500\text{g} \times 0.5}{280.45\ g/mole}$

$N_{AO} = \frac{250\text{ mole}}{280.45}$

$= 0.8914\ mole$

V = $\frac{0.8914\ min^{-1}\ x\ 0.5}{30\text{ min x } 0.0095\ min^{-1} x\ 0.00045\ mol/cm^3}$

= 3475 cm^3

Safety factor = 20% of the computed volume

Therefore, total volume of the reactor = 3475 + 695 = 4170cm^3

Volume of the reactor ≈ 4.2 litter

But volume of the reactor which is cylindrical in shape, therefore, equation of the volume of a cylinder will be applied, V = $\pi r^2 h$ (Ikhazuangbe and Eruotor, 2017).

Assuming internal diameter of $15cm$, radius will be $7.5cm$

Where r = radius of the reactor and h = height of the reactor

Therefore,

4.2L = $\pi\ 7.5^2 cm^2 h$

h = $\frac{4200cm^3}{\pi\ x\ 56..25cm^2}$

$\approx 24cm$

The process configuration that will be considered in this study is shown in Figure 1. The batch reactor will be assumed to be completely mixed and no material will leave the reactor during the operation.

1) Wall thickness of the reactor

The thickness of the reactor was designed using equation (8). The maximum internal design gauge pressure according to Rehan, (2020), is 25bar (10,833.3kpa), and Casting quality factor = 1, temperature coefficient = 0.4, the basic allowable stress for pipe material = 359870kpa, where the sum of mechanical allowances (thread depth) plus corrosion was taken as C = 0mm, since the reactor will be fabricated with stainless steel 316 (Towler and Sinnott, 2008).

Consequently, the pressure design thickness of the cylindrical reactor is presented in Table 5.

2) Design of the Flat End

Since the determination of the thickness of flat plate is dependent on stress analysis of the plates, equation (9) was used, while the design stress of the stainless steel 316 was obtained from Table 2 at 400^{o}C. For flanged-only end, C is 0.17 if corner radius is not more than 3t; otherwise C is 0.1 and D_e is equal to D_i (Sinnott, 2005). The result of the thickness of the flat end is presented in Table 5.

3) Design of stirrer with impellers

Stirring time and speed are the major variables that aid the homogeneity of a reaction and when the stirrer is properly designed and the stirring time and speed determined and adjusted, the quality and yield of the biocrude will be improved (Muhammad and Jalal, 2021). Table 4 was used for the computation of the parameters of the impeller, and the results are presented in Table 5.

4) Design of the heat insulation

The thickness of the insulation material (fiberglass) was designed using equation (11), and the thermal conductivity of the stainless steel and fiberglass were obtained from Tables 3. The maximum amount of design heat produced in the reactor at 400ºC for 30 minute was obtained as 1096W. Therefore, using equation (11) where the thermal conductivity of the fiberglass Type I is $0.044 w/m$ ℃ and that of stainless steel 316 is $16\ w/m$ ℃ (Zaid, 2020), the minimum thickness of the insulation was obtained as 2mm.

Table 5 Configuration of the Batch Reactor Design

Section	Parameters	Equation
	Reactor type	Batch
	Material of the reactor	Stainless steel
	Height of reactor	240mm
	inner diameter of the reactor	150mm
	Reactor capacity	4.2 liter
	Temperature sensor	0 - 400℃
	Pressure gauge	0 – 40bar
	Thickness of the reactor wall	2.2mm
	Outer diameter of the reactor	152mm
	Thickness of the flat end	4.8mm
	Insulation thickness	2mm
	Length of the circle of the reactor	560mm
Stirrer	Impeller diameter (Da)	75mm
	Impeller height from the bottom of the vessel (Zi)	50mm
	Impeller width (W)	15mm
	Impeller length (L)	18.8mm

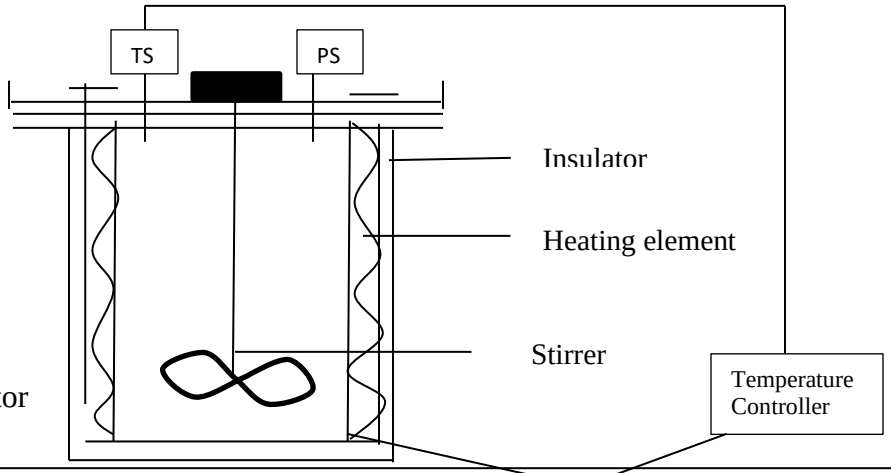

PS = Pressure sensor
TS = temperature sensor

Figure 1 The Batch Reactor

Table 6 Bill of Engineering Measurement and Evaluation

Item	Quantity	Price (N)
Pressure gauge	1	40,000
Pressure valve	1	2,500
Electrical heating element	2 pack	40,000
Control panel & Temperature sensor	1	61,000
Flat plate (5mm)	2	30,000
Flat plate hanger	1	10,000
Fiberglass material	1 bag, 4 wards	20,000
Stainless steel electrode	1 pack	18,000
Production cost (mechanical & electrical)	-	25,000
Miscellaneous		10,000
Stainless steel screw	12	1,200
Pressure gauge cup	1	500
Total		258,200

Two Hundred and Fifty Eight Thousand, Two Hundred Naira only

IV. RESULTS AND DISCUSSION

The process design was carried out isothermal temperature and the percentage compositions of the biogas, biocrude, liquid phase and biochar used were 5wt%, 50wt%, 30wt% and 15wt% respectively, at a ratio of 4:1 between the solvent (water) and the microalgae, according to Eboibi *et al*, (2015); Le *et al*, (2019). The results obtained from the material balance of the mixture of water and microalgae biomass gave a total mass of $2500g$. These are $125g$ of biogas, $1250g$ of biocrude, $750g$ of the liquid phase, and $375g$ of the biochar.

The energy balance of the reactor is also carried out by calculating the heat content of the triglyceride in the mixture, using the mass of the mixture from the material balance which is $2500g$. Therefore, the result of the amount of design heat required in the reactor unit of both the microalgae biomass and water is $1096W$.

The equipment design of the reactor involves the design of the volume, height, wall thickness and the thickness of the insulation material on the refractory covering the electrical heating element. The reactor volume was design as 4.2 liter ($4170cm^3$), which agrees with the reactors used by Hoang *et al*, (2021) and Kandasamy *et al*, (2021) in their research work, when the ratio of the biomass to reactor volume they used is considered, but did not follow the trend of the volume used by Costarizo *et al.*, (2015) and Wang *et al.*, (2018) under the same conditions.

The height of the reactor was designed as $240mm$ which did not agree with the height of the reactor used by Jazrawi *et al*, (2015), who reported that they used a height of 120mm for a 20ml reactor, even though it was reported in their work that approximately 3g sample of the microalgae was used. Other authors whose articles were considered in this work did not report the details of the height of the reactor they used.

The wall thickness of the reactor was designed as $2.2mm$ which is higher than the 1.65mm wall thickness reported by Jazrawi *et al*, (2015). The variance is understandable because the wall thickness is a function of the reactor volume. However, Aprilla *et al.*, (2023) reported in their design of a reactor for the production of Fe_3O_4 Nanoparticles, wall thickness of 1mm. The

thickness of the top flat end was designed separately and was obtained as 4.7mm, to be able to withstand the reactor pressure and prevent possible leakages.
The fiberglass thickness used as insulation material of the reactor was designed as 2mm, but none of the researchers mentioned in this article, reported the details of the insulation material they used for their reactor. However, safety factors were put consideration during the design and fabrication of the insulation of the reactor. Cooling of the reactor will be carried out when the operation is shut down, before the pressure relief valve fitted to the reactor will be opened to vent out the gas.
The entire design and fabrication of this reactor as presented in Table 6, is estimated at Two Hundred and Fifty Eight Thousand, Two Hundred Naira (N258,200) only. Nevertheless, most of the researchers referenced in this article did show the detailed design of the reactor they used; they did not also report the cost of their reactor.

V. CONCLUSIONS

Microalgae biomass is an attractive alternative source for the production of biocrude, and this design of an efficient laboratory-scale batch reactor for its production by hydrothermal liquefaction is of great importance. The results from this study contribute to the body of knowledge for batch processes and biocrude production. The 2.2mm thick batch reactor is designed to operate under safe condition with a maximum design heat production of 1096W, using electrical heating system, insulated with fiberglass of about 2mm thickness. The temperature sensor is designed to measure a maximum temperature of about 400^{o}C inside the reactor, also fitted with a maximum pressure gauge of 40bar, mounted on a top flat end of 4.7mm thickness. This design is economical and will be fabricated using stainless steel 316 material, which has high corrosion and heat resistance.

AUTHOR CONTRIBUTIONS

B.E. Eboibi: Conceptualization, Supervision, review, Validation; P.M.O. Ikhazuangbe: Writing – original draft, review & editing; B. Amabogha: Writing & editing; O.H. Orugba: Supervision, review; Ikalumhe W.O. Mechanical Design &. S.E. Agarri: Supervision.

REFERENCES

Amiri, P. and Arabian, D. (2016). The Effect of Reactor Configuration and Performance on Biodiesel Production from Vegetable Oil. Journal of Applied Biotechnology Reports, 3 (2): 403-411

Aprilia, M.P.; Nandiyanto, A.B.D. and Ragadhita, R. (2023). Design of reactor for the production of Fe_3O_4 nanoparticles. Green and Applied Chemistry, 16: 01- 07.

Barreiro, D.L.; Samori, C.; Terranella, G.; Horiung, U.; Kruse, A. and Prins, W. (2014). Assessing microalgae biofuels via hydrothermal liquefaction. Bioresources Technology, 174: 256–265.

Barreiro, D.L.; Samorì, C.; Terranella, G.; Hornung, U.; Kruse, A. and Prins, W. (2014). Assessing microalgae biorefinery routes for the production of biofuels via hydrothermal liquefaction. Bioresource Technology, 174: 256 - 265.

Chen Z.; Wang L.; Qiu S. and Ge, S. (2018). Determination of Microalgal Lipid Content and Fatty Acid for Biofuel Production. Biomedical Research International, 1503126.

Chen, P.H. and Quinn, J.C. (2021). Microalgae to biofuels through hydrothermal liquefaction: Open-source techno-economic analysis and life cycle assessment. Applied Energy, 289: 1–17.

Costanzo, W.; Jena, U.; Hilten, R.; Das, K. and Kastour, J.R. (2015). Low temperature hydrothermal pretreatment of algae to reduce nitrogen heteroatoms and generate nutrient recycle streams. Algae resources, 12: 377–387.

Eboibi, B.E. (2019). Impact of time on yield and properties of biocrude during downstream processing of product mixture derived from hydrothermal liquefaction of microalga. Biomass Conversion and Biorefinery, 9: 379–387.

Eboibi, B.E.; Lewis, D.M.; Ashmana, P.J. and Chinnasamy, S. (2015). Influence of process conditions on pretreatment of microalgae for protein extraction and production of biocrude during hydrothermal liquefaction of pretreated *Tetraselmis sp*. Royal Society of Chemistry advances, 5: 20193–20207.

Etuk, S.E.; Robert, U.W. and Agbasi, O.E. (2020). Design and performance evaluation of a device for determination of specific heat capacity of thermal insulators. Beni-Suef University Journal of Basic and Applied Sciences, 934: 1 – 7.

Fogler, H.S. (2012). Elements of chemical reaction engineering. PHI Learning limited, New Delhi, 30 – 40.

Geada, P.; Gkelis, S.; Teixeira, J.; Vasconcelos, V.; Vicente, A.A. and Fernandes, B. (2017). Cyanobacterial toxins as a high value-added product. Microalgae-Based Biofuels and Bioproducts, 401-428.

Hao, B.; Xu, D.; Jiang, G.; Ahmed, T.; Jing, S.Z. and Guo, Y. (2021). Chemical reactions in the hydrothermal liquefaction of biomass and in the catalytic hydrogenation upgrading of biocrude. The Royal Society of Chemistry, 23: 1562–1583.

Hoang, A.T.; Ong, H.C.; Fattah, I.M.R.; Chong, C.T.; Cheng, C.K.; Sakthivel, R. and Ok, Y.S. (2021). Progress on the Lignocelluloses Biomass Pyrolysis for Biofuel Production towards Environmental Sustainability. Fuel Process Technology, 223: 1 – 27.

Hu, Y.; Gong, M.; Feng, S.; Xu, C.C. and Bassi, A. (2019). A review of recent developments of pre-treatment technologies and hydrothermal liquefaction of microalgae for bio-crude oil production. Renewable and Sustainable Energy Reviews, 101, 476–492.

Ikhazuangbe, P.M.O. and Eruotor M.O. (2017). Development of High Performance Temperature Controlled Laboratory-Based Diffusivity Device. International Journal of Petroleum and Petrochemical Engineering, 3 (3): 1-6

Iyagba, E.T. (2008). Fundamentals of transport phenomena. Jita Enterprises, Port Harcourt, Nigeria, 31 – 36.

Jazrawi, C.; Biller, P.; He, Y.; Montoya, A.; Ross, A.B. and Maschmeyer, T. (2015). Two-stage hydrothermal liquefaction of a high-protein microalgae. Algae resources, 8, 15 – 22.

Joelianingsih,; Tambunan, A.H. and Nabetani, H. (2014). Reactivity of Palm Fatty Acids for the Non-catalytic Esterification in a Bubble Column Reactor at Atmospheric Pressure. Procedia Chemistry, 9: 182–193.

Kandasamy, S.; Devarayan, K.; Bhuvanendran, N.; Zhang, B.; He, Z.; Narayanan, M.; Mathimani, T.; Ravichandran, S. and Pugazhendhi, A. (2021). Accelerating the production of bio-oil from hydrothermal liquefaction of microalgae via recycled biochar-supported catalysts. Journal of Environmental Chemical Engineering, 9: 1 – 15.

Kumar, A.; Guria, C.; and Pathak, A.K. (2018). Optimal cultivation towards enhanced algaebiomass and lipid production using Dunaliella tertiolecta for biofuel application and potential CO2 biofixation: Effect of nitrogen deficient fertilizer, light intensity, salinity and carbon supply strategy. Energy, 153: 1 – 51.

Le, A.P.P.; Julien, L.; Paul, B. and Adrien, W. (2019). Finding optimal algal/bacterial inoculation ratio to improve algal biomass growth with waste water as nutrient source. African Journals Online, 45 (4): 1–8.

Mahima, J.; Sundaresh, R.K.; Gopinath, K.P.; Rajan, P.S.S.; Arun, J.; Kim, S. and Pugazhendhi, A. (2021). Effect of algae (*Scenedesmus obliquus*) biomass pre-treatment on bio-oil production in hydrothermal liquefaction (HTL): Biochar and aqueous phase utilization studies. Science of the Total Environment, 778: 1–9.

Muhammad, F. and Jalal, S. (2021). A Comparative Study of the Impact of the Stirrer Design in the Stir Casting Route to Produce Metal Matrix Composites. Advances in Materials Science and Engineering, 1 – 15.

Octave, L (2008). Chemical reaction engineering. John Wiley & sons ltd, Singapore, 83 – 85.

Rehan, A.K. (2020), Pipe thickness calculation as per ASME B31.3, Pipe thickness calculator, piping design basics, piping stress analysis, piping stress basics.

Sinnott, R. K. (2005). Chemical Engineering Design. Butterworth-Heinemann, London, 811 – 820.

Song, W.; Wang, S. and Guo, Y. (2015). A Review of the Biofuel Yield in Hydrothermal Liquefaction of Different Microalgae. International Conference on Advances in Energy and Environmental Science, 1504 – 1509.

SundarRajan, P.; Gopinath, K.P.; Arun, J. GracePavithra, K.; Joseph, A. and Manasa, S. (2021). Insights into valuing the aqueous phase derived from hydrothermal liquefaction. Renewable and Sustainable Energy Reviews, 144: 1–15.

Tian, C.; Li, B.; Liu, Z.; Zhang, Y. and Lu, H. (2014). Hydrothermal liquefaction for algal biorefinery: A critical review. Renewable and Sustainable Energy Reviews, 38: 933–950.

Tian, S.L.; Khan, A.; Zheng, W.N.;, Song, L.; Liu, J.H.; Wang, X.Q. and Li, L. (2022). Efects of Chlorella extracts on growth of Capsicum annuum L. seedlings. Scientific report, 12 (15455).

Towler, G. and Sinnott, R. (2008). Chemical Engineering Design: Principles, Practice and Economics of Plant and Process Design. Butterworth-Heinemann, London, 263 – 264.

Vardon, D.R.; Sharma, B.K.; Blazina, G.V.; Rajagopalan, K. and Strathmann, T.J. (2012). Thermochemical conversion of raw and defatted algae biomass via hydrothermal liquefaction and slow pyrolysis. Bioresources Technology, 109: 178–187.

Wang, S.; Zhao, S.; Cheng, X.; Qian, L.; Barati, B.; Gong, X.; Cao, B. and Yuan, C. (2021). Study on two-step hydrothermal liquefaction of macroalgae for improving bio-oil. Bioresource Technology, 319: 1 – 9.

Wang, W.; Xu, Y.; Wang, X.; Zhang, B.; Tian, W. and Zhang, J. (2018). Hydrothermal liquefaction of microalgae over transition metal supported TiO2 catalyst. Bioresource Technology, 250: 474–480.

Xu, Y.; Hu, Y.; Peng, Y.; Yao, L.; Dong, Y.; Yang, B. and Song, R. (2019). Catalytic pyrolysis and liquefaction behavior of microalgae for bio-oil production. Bioresource Technology, pp. 1 – 37.

Zaid, R. (2020). Pipe insulation

Zhu, X.; Phinney, D.M.; Paluri, S. and Heldman, D.R. (2018). Prediction of Liquid Specific Heat Capacity of Food LipidS. Journal of food sciences, 0 (0): 1 – 6.